STUDIES ON SPENT FUEL DISSOLUTION BEHAVIOR
UNDER YUCCA MOUNTAIN REPOSITORY CONDITIONS

C. N. Wilson

C. J. Bruton[a]

Pacific Northwest Laboratory
Richland, Washington 99352

(a) Lawrence Livermore National Laboratory
     Livermore, California 94550

STUDIES ON SPENT FUEL DISSOLUTION BEHAVIOR
UNDER YUCCA MOUNTAIN REPOSITORY CONDITIONS

C. N. Wilson

C. J. Bruton[a]

PNL-SA--16832

DE89 017242

July 1989

(a) Lawrence Livermore National Laboratory
     Livermore, California 94550

DISTRIBUTION OF THIS DOCUMENT IS UNLIMITED

MASTER

STUDIES ON SPENT FUEL DISSOLUTION BEHAVIOR
UNDER YUCCA MOUNTAIN REPOSITORY CONDITIONS

C. N. Wilson
Pacific Northwest Laboratory

C. J. Bruton
Lawrence Livermore National Laboratory

ABSTRACT

Nuclide concentrations measured in laboratory tests with PWR spent fuel specimens in Nevada Test Site J-13 well water are compared to equilibrium concentrations calculated using the EQ3/6 geochemical modeling code. Actinide concentrations in the laboratory tests reach steady-state values lower than those required to meet Nuclear Regulatory Commission (NRC) release limits. Differences between measured and calculated actinide concentrations are discussed in terms of the effects of temperature (25°C to 90°C), sample filtration, oxygen fugacity, secondary phase precipitation, and the thermodynamic data in use. The concentrations of fission product radionuclides in the laboratory tests tend to increase continuously with time, in contrast to the behavior of the actinides.

1.0 INTRODUCTION

The Yucca Mountain Project of the U.S. Department of Energy is studying the potential dissolution and radionuclide release behavior of spent fuel in a candidate repository site at Yucca Mountain, Nevada. The repository horizon under study lies in the unsaturated zone 200 to 400 meters above the water table. With the exception of C-14, which may migrate in a vapor phase,[1] and possibly I-129, the majority of long-lived radionuclides present in spent nuclear fuel will be transported from a failed waste package in the repository via dissolution or suspension in water in the absence of a major geological event such as volcanism.

1

Spent fuel will not be contacted by liquid water infiltrating the rock until several hundred years after disposal when the repository has cooled to below the 95°C boiling temperature of water at the repository elevation. The potential dissolution behavior of spent fuel during the repository post-thermal period is being studied using geochemical models and laboratory tests with actual spent fuel specimens.* Selected initial results from these studies are discussed in the present paper.

2.0 LABORATORY TESTS

Three spent fuel dissolution test series have been conducted in laboratory hot cells using spent fuel specimens of various configurations. Results from the Series 2 and Series 3 tests with bare fuel particles are discussed in the present paper. The Series 2 tests used unsealed fused silica test vessels and were run for five cycles in air at ambient hot cell temperature (25°C). The Series 3 tests used sealed stainless steel vessels and were run for three cycles at 25°C and 85°C. Each test cycle was started in fresh Nevada Test Site J-13 well water and was about six months in duration. Periodic solution samples were taken during each test cycle and the sample volume was replenished with fresh J-13 water. Five bare fuel specimens tested in these two test series are identified in Table 1 and the test configurations are shown in Figure 1. The composition of J-13 well water[2] is given in Table 2. Additional information on the laboratory tests is provided in references 3 and 4.

all oxidized → no further consumption of oxygen dissolved in leachates

2.1 Actinide Results

Actinide concentrations (U, Np, Pu, Am and Cm) measured in solution samples rapidly reached maximum levels during the first test cycle and then generally dropped to lower steady-state levels in later test cycles. The concentrations of uranium and the activities of Pu-239+240 and Am-241 measured in 0.4 μm filtered solution samples are plotted in Figure 2. The initial concentration peaks are attributed to dissolution of more readily soluble UO_{2+x} oxidized phases present initially at the fuel particle sur-

Table 1. Bare Fuel Test Identification

Identification	Description	Starting Fuel Wt. (g)
HBR-2-25	Series 2, H. B. Robinson Fuel, 25°C	83.10
TP-2-25	Series 2, Turkey Point Fuel, 25°C	27.21
HBR-3-25	Series 3, H. B. Robinson Fuel, 25°C	80.70
HBR-3-85	Series 3, H. B. Robinson Fuel, 85°C	85.55
TP-3-85	Series 3, Turkey Point Fuel, 85°C	86.17

faces, and to kinetic factors limiting the nucleation and growth of secondary phases that may ultimately control actinide concentrations at lower levels.

Uranium (U) concentrations at 25°C were lower in the Series 3 tests than in the Series 2 tests, and with the exception of the Cycle 1 data, U concentrations in the 85°C Series 3 tests were lower than those in the 25°C tests. The very low U concentrations measured during Cycle 1 of the HBR-3-85 test are attributed to a vessel corrosion anomaly. In the later cycles of the Series 2 tests, U concentrations tended to stabilize at steady-state levels of about 1 to 2 µg/ml. In Cycles 2 and 3 of the Series 3 tests, U concentrations stabilized at about 0.3 µg/ml at 25°C and about 0.15 µg/ml at 85°C. Precipitated crystals of the calcium-uranium-silicates, uranophane (Figure 3) and haiweeite, and possibly the uranium-silicate soddyite, were found on filters used to filter cycle termination rinse solutions from both 85°C tests. Phase identifications were based on examinations by X-ray diffraction and microanalysis in the SEM[4]. Secondary phases controlling actinide concentrations other than U were not found.

The 0.4 µm filtered Pu-239+240 solution activities measured in Cycles 2 through 5 of the TP-2-25 test generally ranged from about 100 to 200 pCi/ml (Figure 2). Activities as low as about 20 pCi/ml were measured in the HBR-2-25 test. During Cycles 2 and 3 of the HBR-3-25 test, activities varied from about 60 to 100 pCi/ml. A value of 100 pCi/ml, which corresponds to a Pu concentration of about 4.4×10^{-9} M (M = molarity), would appear to be a reasonable estimate of steady-state Pu-239+240 activities in 0.4 µm filtered solutions in the 25°C tests. Significantly lower activities on the order of 1 pCi/ml were measured in the 85°C tests. The lower activities at 85°C may result from enhanced nucleation and growth of secondary phases at the higher temperature that limit Pu concentration.
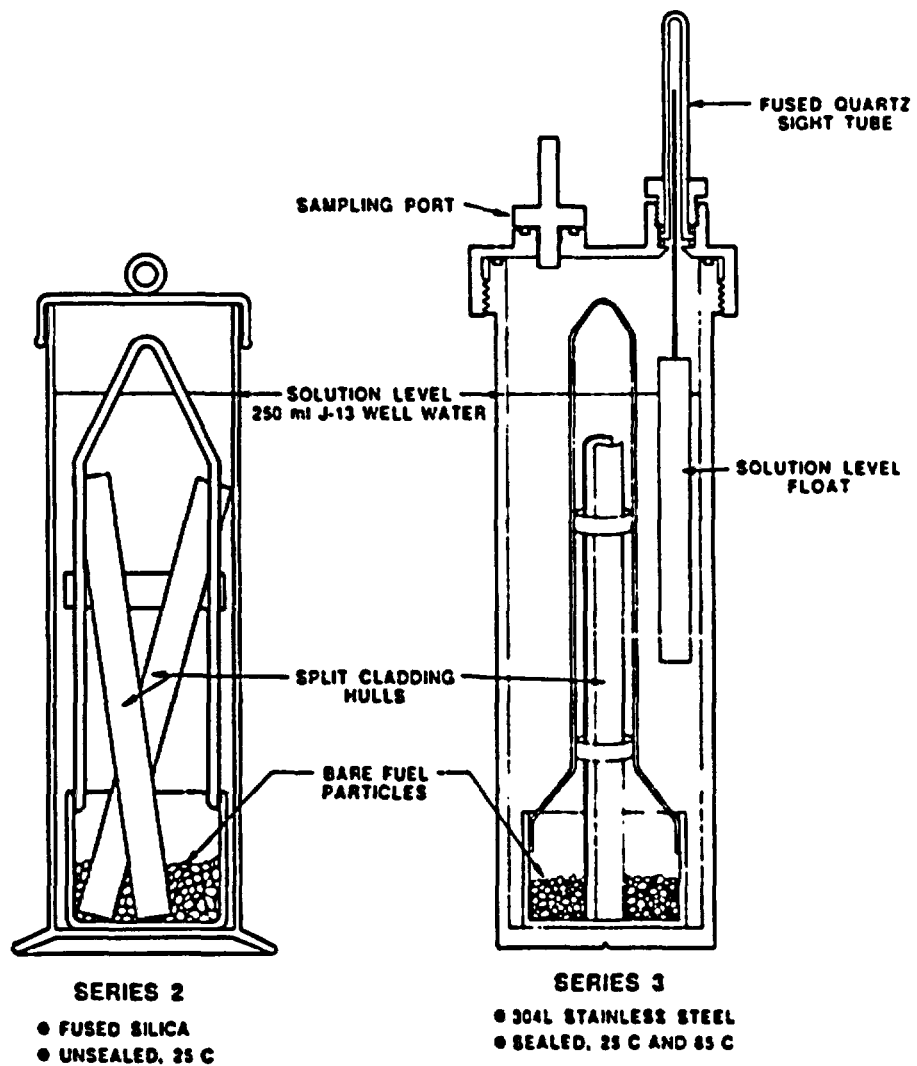
Figure 1. Test Configurations for the Series 2 and Series 3 Bare
Fuel Dissolution Tests.

Selected solution samples were centrifuged through membrane
filters that provide an estimated filtration size of approxi-
mately 2 nm.* Filtering to 2 nm caused Pu-239+240 activities to

---

* Amicon Corporation Model CF-25 centrifuge membrane cone filter.

Table 2. J-13 Well Water Analysis[2]

Component	Concentration (μg/ml)	Component	Concentration (μg/ml)
Li	0.042	Si	27.0
Na	43.9	F	2.2
K	5.11	Cl	6.9
Ca	12.5	NO_3	9.6
Mg	1.92	SO_4	18.7
Sr	0.035	HCO_3	125.3
Al	0.012		
Fe	0.006	pH	7.6

decrease by about 20 to 40%. No significant differences between
unfiltered and 0.4 μm filtered Pu activities were noted. The
0.4 μm filtered sample data are considered the most significant
relative to radionuclide release because larger particles prob-
ably would not be transported by water, whereas colloidal par-
ticles greater than 2 nm may remain in stable suspension and be
transported by water movement.

Steady-state Am-241 activities on the order of 100 pCi/ml, cor-
responding to Am concentrations of about 1.5×10^{-10} M, were mea-
sured in 0.4 μm filtered samples during Cycles 2 and 3 of the
TP-2-25 and HBR-3-25 tests. The 100 pCi/ml value would appear to
be a conservative estimate for Am-241 activity at steady-state
and 25°C considering that activities on the order of 10 pCi/ml
were measured during Cycles 2, 4 and 5 of the HBR-2-25 test.
Much lower 0.4 μm filtered Am-241 activities of about 0.3 pCi/ml
were measured during Cycles 2 and 3 of the two 85°C tests. The
effects of both 0.4 μm and 2 nm filtration were in general
greater for Am-241 than for Pu-239+240. Association of Am with
an apparent suspended phase is suggested by unfiltered data from
the 85°C tests plotted as dashed lines in Figure 2, and by a
relatively large fraction of 0.4 μm filtered Am-241 activity
removed by 2 nm filtration (not shown). Cm-244 activity measured
in most samples was similar to that measured for Am-241 in each
of the tests. However, Cm-244 alpha decays with a 18-year half-
life to Pu-240 and will not be present during the repository
post-thermal period.

Measured Np-237 activities in most samples were generally not
much greater than the detection limit of 0.1 pCi/ml and were
below detection limits in several samples. Measured Np-237
activities showed very little dependence on temperature, vessel

5
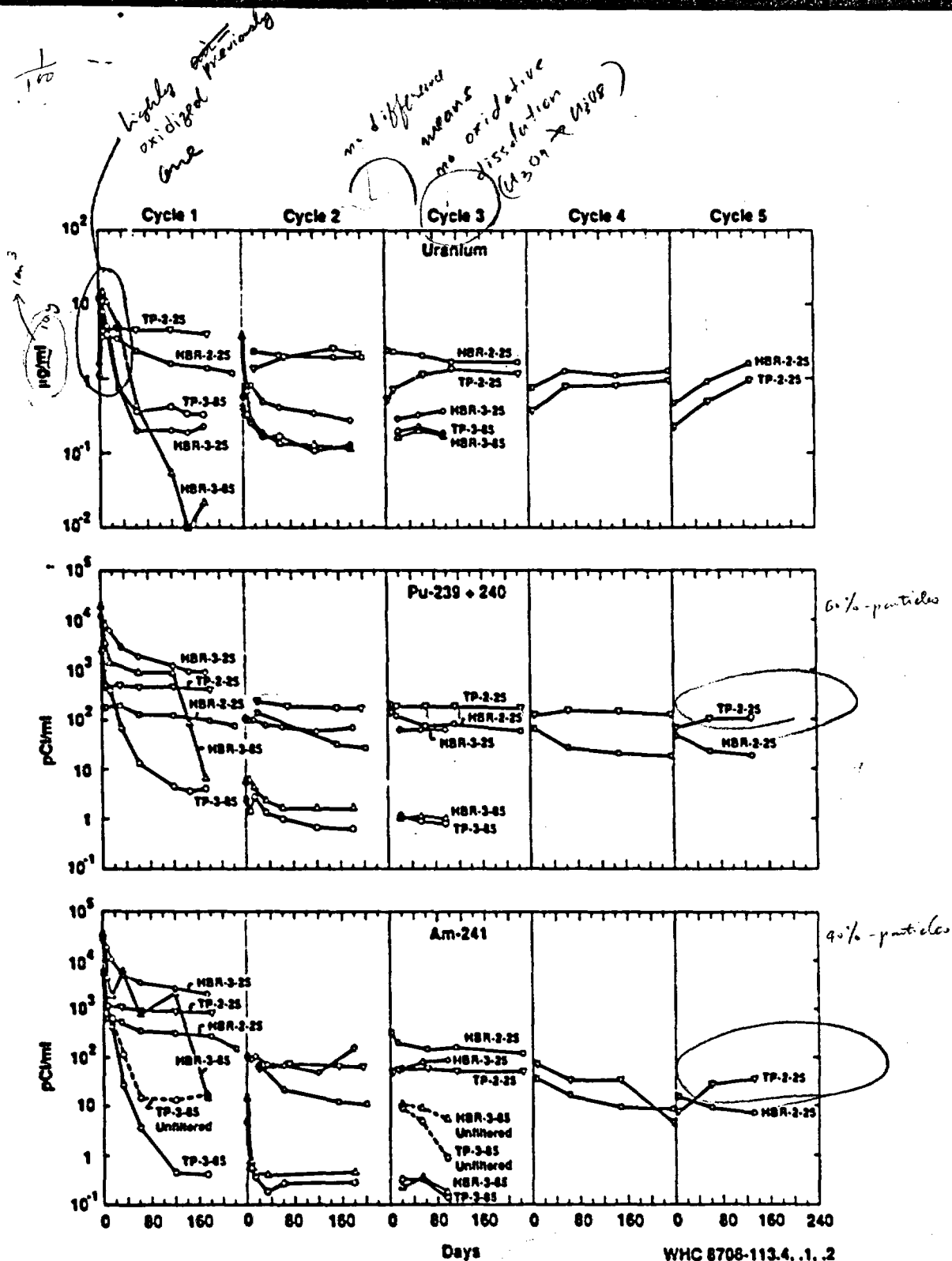
Figure 2. Uranium Concentrations (top), Pu-239+240 Activities (center) and Am-241 Activities (bottom) Measured in 0.4 μm Filtered Solution Samples.
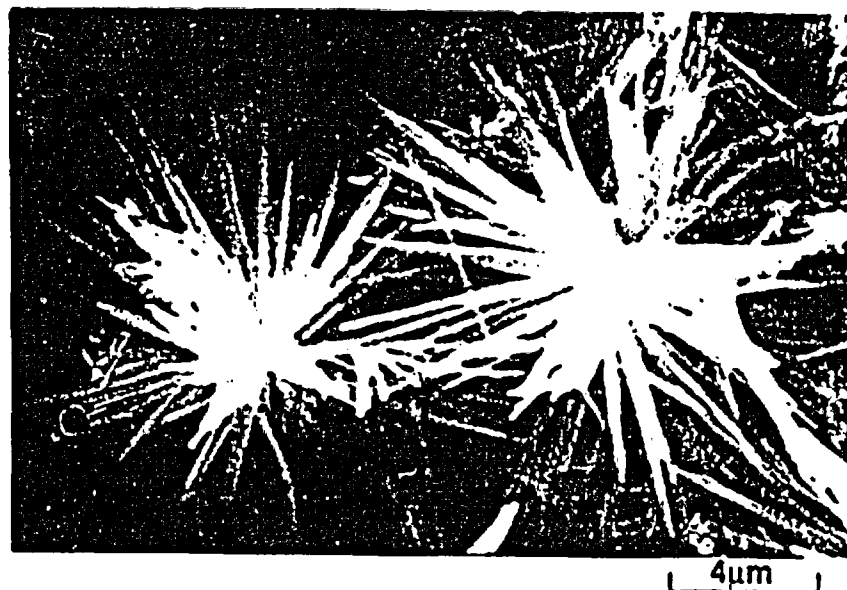
Figure 3. Acicular Crystals of Uranophane Formed on Spent Fuel
Grains in the 85°C Series 3 Tests.

type or sample filtration. Following initially higher values at
the beginning of Cycle I, Np-237 activities generally ranged from
0.1 to 0.5 pCi/ml.

2.2 Fission Product Results

Specimen inventory fractions of the fission product radionuclides
Cs-137, Sr-90, Tc-99 and I-129 measured in solution are plotted
in Figure 4 for the HBR-2-25 and HBR-3-85 tests. Each data point
represents the fraction of the ORIGEN-2 calculated specimen
inventory in solution on the sample date plus the inventory frac-
tion calculated to have been removed in previous samples from the
test cycle. During Cycle 1 of the HBR-3-85 test, Tc-99 fell to
below detectable levels as a result of the corrosion anomaly that
occurred in this test. Cycle 1 Cs-137 gap inventory release was
about 0.7% from the HBR fuel and is therefore off-scale in Fig-
ure 4. Sr-90 was not measured during Cycle 1 of the Series 2
tests, and appeared to be limited by association with an unknown
precipitated phase in the 85°C tests.

The inventory fractions of Cs-137, Sr-90, Tc-99 and I-129 in
solution increased continuously with time, with the exception of
the anomalous precipitation of Tc-99 in Cycle 1 of the HBR-3-85

7

Figure 4.   Inventory Fractions of Cs-137, Sr-90, Tc-99 and I-129
Measured in Solution in the HBR-2-25 Test (top) and
in the HBR-3-85 Test (bottom). Approximate annual
fractional release rates are listed for each nuclide
during the last cycle plotted.

8

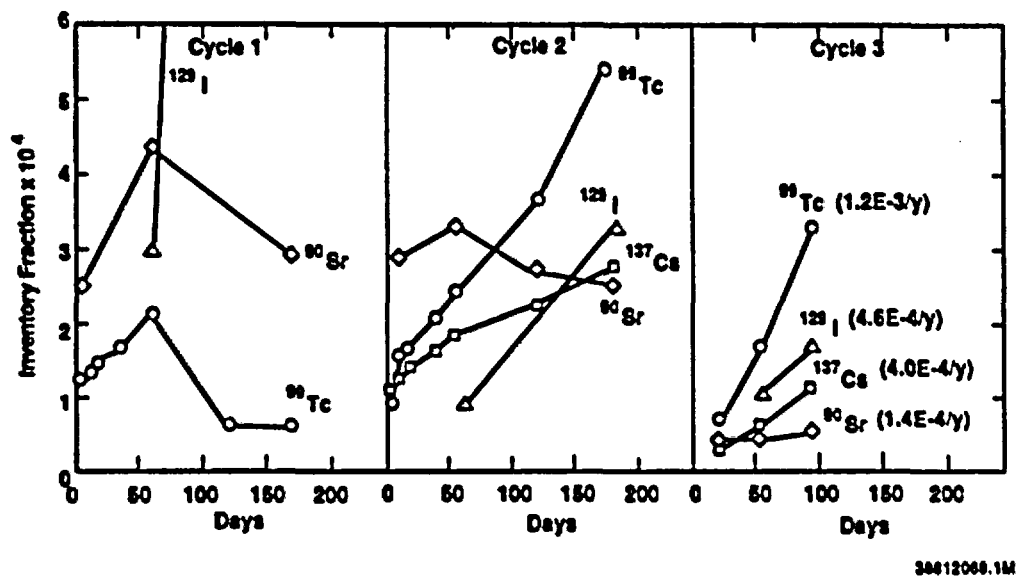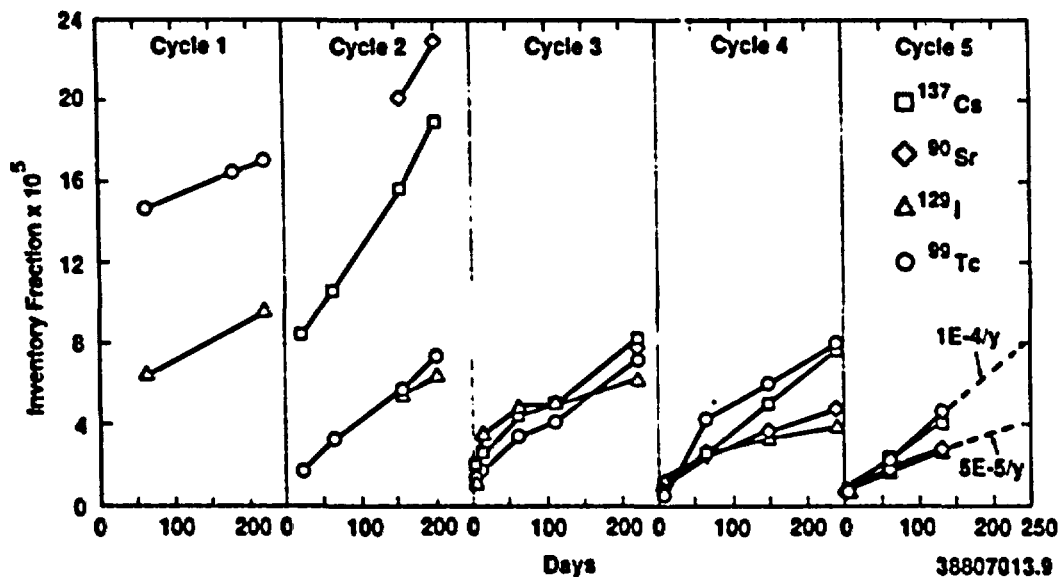test and the limit on Sr-90 activity in solution at 85°C. The continuous release rates of the fission products in units of inventory fraction per year are given in Figure 4 for the final cycle of the two tests. Because the actual quantity of fuel matrix dissolution and precipitation of actinides was not measured, it is not known to what degree the continuous fission product release resulted from preferential leaching of grain boundaries where fission products are thought to concentrate during irradiation. Whether as a result of increased matrix dissolution or increased grain boundary leaching, the soluble fission product release rate is greater in the later test cycles at the higher temperature.

3.0 GEOCHEMICAL MODELING

3.1 Actinide Concentrations in Solution

Spent fuel dissolution in J-13 well water was simulated using the geochemical modeling code EQ3/6[5] to determine whether steady-state actinide concentrations measured in the tests could be related to the precipitation of actinide-bearing solids. Version 3245 of the EQ3/6 code and version 3270R13 of the supporting thermodynamic database were used to simulate spent fuel dissolution at 25°C and 90°C assuming atmospheric CO_2 gas fugacity and two different O_2 gas fugacities of $10^{-0.7}$ (atmospheric) and 10^{-12} bars (see later discussion). The simulation process is described in more detail elsewhere.[6] The computer simulations yield: 1) the sequence of solids that precipitate and sequester elements released during spent fuel dissolution; and 2) the corresponding elemental concentrations in solution. Approximate steady-state actinide concentrations measured at 25°C and 85°C in the Series 3 laboratory tests are compared in Table 3 to concentrations of actinides in equilibrium with the listed solids as calculated in the EQ3/6 simulations. Comparisons of simulation results with experimental results are being used to determine the adequacy of the thermodynamic database and to identify additional aqueous species and minerals for which data are needed.

Uranium (U) concentrations in the simulations vary as a function of the secondary U-bearing precipitates. The following sequence of mineral assemblages are predicted to precipitate and sequester U as increasing amounts of spent fuel dissolve: haiweeite, haiweeite plus soddyite, soddyite, soddyite plus schoepite, and schoepite. The relative compositions of these phases and of U-bearing phases that were observed in residues from the 85°C laboratory tests are shown in Figure 5. Unique, and steadily increasing, concentrations of U in solution are related to each

9

Handwritten top:

$10 \, \mu g/mL$

$= \dfrac{10 \times 10^{-6} \times 1000 \times}{238} = 42 \times 10^{-6} \, M$

$= 4.2 \times 10^{-5} \, M$

$\dfrac{4.2 \times 10^{-5}}{10^{-7.2}} \cong 6.3 \times 10^{-8}$

$\sim 10^3$

$10^{-9} \, M/l \; Np$

$2.37 \times 10^{-9} \, g/1mcc$

$2.37 \times 10^{-10} \, g/ml$

$2.37 \times 10^{-10} \, g/g$

$2.37 \times 10^{-9} \, mg/g$

$0.4 \, PCi/ml$

$1 \, PCi = \dfrac{10}{4} \times 2.37 \times 10^{-10} \, g$

$= 5.9 \times 10^{-11} \, g$

Table 3. Comparison of Measured and Predicted Actinide Concentrations (log M)

Actinide	Measured(a) 25°C	85°C	EQ3/6(b) 25°C -0.7	-12.0	90°C -0.7	-12.0	Phase
U	-5.9	-6.2	-7.2/-7.0	-7.1/-6.9	-8.8/-7.6	-8.5/-7.5	H
			-7.0/-6.9	-6.9/-6.8	-7.6	-7.5	H + S
			-6.9/-4.3	-6.8/-4.2	-7.6/-6.0	-7.5/-5.9	S
			-4.3	-4.2	-6.0	-5.9	S + Sch
			-4.2	-4.1	-6.0/-5.8	-5.8/-5.6	Sch
Np	-8.9	-9.1	-6.2	-9.0	-5.2	-8.0	NpO$_2$
Pu	-8.4	-10.4	-12.4	-13.8	-11.9	-14.6	PuO$_2$
			-4.3	-5.7	-4.2	-6.9	Pu(OH)$_4$
Am	-9.8	-12.3	-8.3	-8.3	..	..	Am(OH)CO$_3$
			..	..	-8.4	-8.4	Am(OH)$_3$
Cm	-11.3	-14.3	Cm not in thermodynamic database				

(a) Series 3 tests, 0.4 μm filtered.
(b) At oxygen fugacities log f_{O2} = -0.7 (atmospheric) and log f_{O2} = -12.0 with solubility control by precipitated secondary phases as listed. H = haiweeite; S = soddyite; Sch = schoepite. All phases are in crystalline state except Pu(OH)$_4$ which is amorphous.
* -7.2/-7.0 refers to a range in concentration from -7.2 to -7.0.

mineral assemblage. The concentration of U varies not only as the precipitates vary, but also during the precipitation of a single mineral, such as soddyite, because of changes in the pH and overall chemical characteristics of the fluid. As previously discussed, uranophane, haiweeite, and possibly soddyite were found in the 85°C Series 3 tests. Unfortunately, reliable thermodynamic data for uranophane are not available, which complicates comparison of the laboratory test results to the calculated solubility limits. Haiweeite, a Ca-U-silicate like uranophane, is predicted to precipitate at U concentrations that are lower than the measured steady-state values. In the absence of data for uranophane, the experimental concentrations of U would appear to be consistent with the precipitation of soddyite at both 25°C and 90°C in the simulations.

Handwritten bottom:

$25°C \qquad \dfrac{U}{Pu} = \dfrac{10^{-5.9}}{10^{-8.4}} = \dfrac{1.3 \times 10^{-6}}{4.0 \times 10^{-9}} = 325$

$85°C \qquad \dfrac{U}{Pu} = \dfrac{10^{-6.2}}{10^{-14.4}} = \dfrac{6.3 \times 10^{-7}}{4.0 \times 10^{-11}} = 1.6 \times 10^4$

$10^{-8.4} \, mole/l$

$\dfrac{10^{-8.4} \times 240 \times 4/4}{1.1 \times 10^{-11} \, g} \; (25cc)$

$PCi \quad 2.2 \times 10^{-7} \div 10^{-11}$

$2.2 \times 10^{4} \, PCi$

$= \dfrac{22400}{250} \cdot 250$
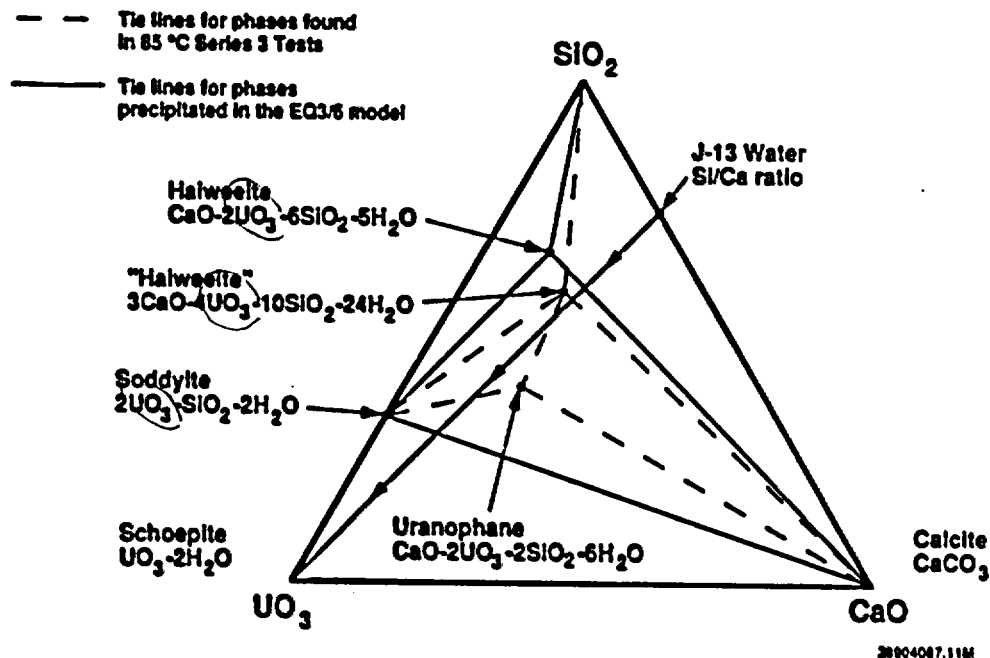
$= 90 \, PCi/cc$

10

Figure 5. Relative Compositions (mole %) of U-bearing Phases Indicated as Controlling U Concentration in the EQ3/6 Simulation and for which Indications were Observed in the 85°C Series 3 Tests.

Neptunium concentration is controlled by equilibrium with NpO_2 in the simulations. However, the predicted concentration of Np is highly dependent on solution Eh and pH.[7] The O_2 fugacity in the simulations was reduced from $10^{-6.7}$ bars to 10^{-12} bars in order to produce good agreement between the measured and predicted concentrations of Np at 25°C. An O_2 fugacity of 10^{-12} bars may correspond to conditions at the fuel surface in an otherwise oxygenated system (i. e. contains an air cap) that is poorly buffered. Eh was not measured during the laboratory tests, and redox equilibrium may not have been established among the various species and phases within the sealed stainless steel vessels. An oxygen fugacity of 10^{-12} bars over-estimates Np concentration at 90°C, however, because the experimental data do not reflect predicted increases in Np concentration with temperature. The thermodynamic data for Np and other actinides must, consequently, be critically evaluated at elevated temperature.

Significant differences exist between measured and predicted Pu and Am concentrations in Table 3. Measured Am concentrations may have been lower than those predicted because of Am removal from

11

solution by phases such as lanthanide precipitates that were not accounted for in the EQ3/6 simulations. Another possible mechanism controlling Am concentration not accounted for in the simulation may have been sorption. Although $Am(OH)CO_3$ is predicted to control Am concentration at 25°C and $Am(OH)_3$ precipitates at 90°C, the Am concentration in equilibrium with both phases is about the same.

Predicted Pu concentrations in equilibrium with crystalline PuO_2 at both temperatures and oxygen fugacities are much lower than those measured. Pu concentrations measured at 25°C are similar to those reported by Rai and Ryan[8], who measured the solubility of PuO_2 and hydrous $PuO_2 \cdot xH_2O$ in water for periods of up to 1300 days at 25°C. At a pH of 8, which was the extrapolated lower limit of their data and the approximate pH in the Series 2 and 3 tests, they reported that Pu concentrations ranged from about $10^{-7.4}$ M, where amorphous $PuO_2 \cdot xH_2O$ was thought to control concentration, down to about 10^{-9} M where aging of the amorphous material produced a more (but incompletely) crystalline PuO_2 that was thought to control concentration. Concentrations of Pu in equilibrium with amorphous $Pu(OH)_4$, calculated in recognition of the fact that an amorphous or less crystalline phase is more likely to precipitate than crystalline PuO_2, are listed in Table 3. Measured Pu concentrations would be expected to fall between the equilibrium concentrations for PuO_2 and $Pu(OH)_4$, becoming closer to PuO_2 with aging. Equilibrium with amorphous $Pu(OH)_4$ and crystalline PuO_2 at O_2 fugacities of $10^{-0.7}$ and 10^{-12} bars yields predicted Pu concentrations that bracket measured results at both 25°C and 85°C.

3.2 Sources of Discrepancy Between Measured and Predicted Results

Discrepancies between measured and predicted concentrations are to be expected considering database limitations and uncertainty in the interpretation of measured apparent steady-state actinide concentrations. Care must be taken in interpreting the 90°C simulation results because insufficient data exist to accurately calculate the temperature-dependence of the thermodynamic properties of many radionuclide-bearing solids and solution species. The 3270 thermodynamic database is constantly updated through inclusion of new and revised thermodynamic data and the selection of a consistent set of aqueous complexes for each chemical element. Puigdomenech and Bruno[9] have constructed a thermodynamic database for U minerals and aqueous species that they showed to be in reasonable agreement with available experimental solubility data in systems in which U is complexed by OH^- and $CO_3^=$. The 3270 database contains many of the same aqueous species and

12

minerals, but Puigdomenech and Bruno have included recent data for aqueous uranyl hydroxides from Lemire[10] which are not yet in the EQ3/6 database. Future plans include a critical evaluation of simulations of spent fuel dissolution made using the Puigdomenech and Bruno U database, and comparison with simulations made using the latest version of the EQ3/6 database. Inclusion of standard Nuclear Energy Agency (NEA) data for U minerals and species will also help to standardize future databases.

Until the U database is better established, calculated U concentrations must be recognized as preliminary and speculative. Simulation results can be used as a vehicle for identifying geochemical trends and studying the interactions between solid precipitation and elemental concentrations in solution. Seemingly small changes in the thermodynamic database can have potentially large impacts on predictions. For example, U concentrations calculated to be in equilibrium with schoepite using version 3270 of the EQ3/6 database are radically lower than those predicted in 1987[6] using an older database. The species $(UO_2)_3(OH)_7^-$ and $(UO_2)_2(OH)_3CO_3^-$ were omitted from version 3270 of the EQ3/6 database because their validity was questioned. $UO_2(CO_3)_2^{-2}$ and $UO_2(CO_3)_3^{-4}$ were left as the only dominant U species in solution throughout the EQ3/6 simulations. U concentrations accordingly remain lower during U mineral precipitation, especially schoepite, than in the previous 1987 calculations. Future work must address the sensitivity of the results to variations in thermodynamic data and the choice of a self-consistent set of aqueous species for elements of interest.

Comparisons between experimental results and predictions in Table 3 are predicated on the assumption that the listed solid phases precipitate from solution and control the solution composition. Except for some U-bearing minerals, no minerals containing radionuclides have been identified in the laboratory tests. Detection and characterization of actinide-bearing secondary phases may be difficult because of the extremely small masses of these actinides involved. Precipitates limiting actinide concentrations in the laboratory tests may also be amorphous, colloidal, or in some other less-than-perfect crystalline state. For instance, Rai and Ryan[8] observed that early Pu precipitates tend to be hydrated oxides which undergo aging to more crystalline solids. The concentrations of the affected actinides would, therefore, gradually decrease as aging progresses.

The chemistry of trivalent Am and Cm can be expected to be almost identical to that of the light lanthanide fission product elements which are present in much greater concentrations in

spent fuel than are Am and Cm. Am and Cm may, therefore, be present in dilute solid solution with secondary phases formed by the lanthanides, which would result in lower measured solution concentrations than predicted for Am based on equilibration with $Am(OH)CO_3$ or $Am(OH)_3$. Pu and Np, and possibly Am and Cm, may also have been incorporated at low concentrations in solid solution with the U-bearing precipitates or other secondary phases. Efforts are planned to separate crystals of uranophane from test residues and to perform radiochemical analyses of these crystals to check for incorporation of other radionuclides. Sorption of actinides on colloids or other surfaces such as the fuel or test hardware may also control solution concentrations, but the impact of sorption was not considered in the simulations. Other factors, such as local variations in redox potential, may also contribute to differences between measured and predicted solubilities.

As it is not currently reasonable to expect a geochemical model to predict accurately the effects of all potential concentration-controlling processes over thousands of years, we hope to use modeling predictions to establish upper limits, or conservative estimates, of radionuclide concentrations over time. Lower limits to radionuclide concentrations imposed by solid precipitation are also of interest, however, as a baseline for further calculations, and because radionuclide concentrations may be expected to approach the lower limits over extended time periods. Accordingly, we assume in this paper that the actinide concentrations are controlled by the most stable and insoluble precipitates for which data are available. The consequences of precipitation of progressively less stable precipitates will be explored in future calculations, and upper limits of radionuclide concentrations controlled by solid precipitation will be estimated. In the case of Pu, for example, we have begun to explore the upper limits to Pu concentration as controlled by the precipitation of amorphous $Pu(OH)_4$. Comparison of modeling results with experimental results helps to identify phenomena which may revise our estimates of concentration limits. Processes such as sorption and aging of solids to forms of increasing crystallinity tend to lower element concentrations in solution, and increase the conservative nature of our estimates. However, consideration of colloid formation and colloid migration with the fluid phase may lead to an increase in our estimates of mobile concentrations over those made considering precipitation phenomena alone.